

Long-Term and Clinically Relevant Full-Thickness Human Skin Equivalent for Psoriasis

Smriti Singh,* Yvonne Marquardt, Rahul Rimal, Akihiro Nishiguchi, Sebastian Huth, Mitsuru Akashi, Martin Moeller, and Jens M. Baron*

Cite This: *ACS Appl. Bio Mater.* 2020, 3, 6639–6647

Read Online

ACCESS |

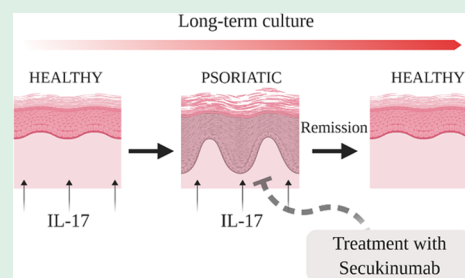
Metrics & More

Article Recommendations

Supporting Information

ABSTRACT: Psoriasis is an incurable, immune-mediated inflammatory disease characterized by the hyperproliferation and abnormal differentiation of keratinocytes. To study in depth the pathogenesis of this disease and possible therapy options suitable, pre-clinical models are required. Three-dimensional skin equivalents are a potential alternative to simplistic monolayer cultures and immunologically different animal models. However, current skin equivalents lack long-term stability, which jeopardizes the possibility to simulate the complex disease-specific phenotype followed by long-term therapeutic treatment. To overcome this limitation, the cell coating technique was used to fabricate full-thickness human skin equivalents (HSEs). This rapid and scaffold-free fabrication method relies on coating cell membranes with nanofilms using layer-by-layer assembly, thereby allowing extended cultivation of HSEs up to 49 days. The advantage in time is exploited to develop a model that not only forms a disease phenotype but can also be used to monitor the effects of topical or systemic treatment. To generate a psoriatic phenotype, the HSEs were stimulated with recombinant human interleukin 17A (rhIL-17A). This was followed by systemic treatment of the HSEs with the anti-IL-17A antibody secukinumab in the presence of rhIL-17A. Microarray and RT-PCR analysis demonstrated that HSEs treated with rhIL-17A showed downregulation of differentiation markers and upregulation of chemokines and cytokines, while treatment with anti-IL-17A antibody reverted these gene regulations. Gene ontology analysis revealed the proinflammatory and chemotactic effects of rhIL-17A on the established HSEs. These data demonstrated, at the molecular level, the effects of anti-IL-17A antibody on rhIL-17A-induced gene regulations. This shows the physiological relevance of the developed HSE and opens venues for its use as an alternative to *ex vivo* skin explants and animal testing.

KEYWORDS: human skin equivalents, scaffold free, psoriasis, IL-17A, secukinumab



INTRODUCTION

Psoriasis is a chronic immune-mediated inflammatory disorder mainly affecting the skin of 2–3% of the general population.¹ Histologically, it is characterized by raised, well-demarcated, erythematous oval plaques. Psoriatic plaques are characterized by an abnormal proliferation and differentiation of keratinocytes, leading to epidermal hyperplasia and results in the reduction or complete absence of the epidermal granular layer. This causes incomplete cornification of the keratinocytes with retention of nuclei (parakeratosis) in the stratum corneum. On the other hand, compared to the normal skin, the mitotic rate of the basal keratinocytes is increased. This gives rise to thickened epidermis.² Since, in psoriasis, premature cell death is combined with accelerated keratinization, late differentiation markers of keratinocytes such as profilaggrin and loricrin are downregulated. Moreover, keratinocyte differentiation markers such as keratin (K) 1 and 10 are reduced, while an increase in expression of proteins KALP/elafin, K6, K16, and K17, which are absent in healthy skin, are expressed. Pathologically, immune cells infiltrate the dermis and epidermis of the psoriatic lesion. This involves the innate and adaptive immune

systems, where dendritic cells (DCs) and T cells, among other cells, play a major role.^{2,3} Due to the presence of CD4⁺ T_h1 and CD8⁺ cytotoxic T cells type 1 (Tc1), tumor necrosis factor (TNF)- α , high levels of interferon (IFN)- γ , and IL-12 in psoriatic lesions, initially, psoriasis was considered to be a T helper cell type 1 (T_h1) cell-mediated disease. A “type 1” inflammatory environment is created by the interaction of T cells with DCs, subsequently releasing T_h1-type cytokines. Lately, an added role of T_h17 cells and their main effector cytokines IL-17A, IL-17F, IL-21, and IL-22 as well as a granulocyte-macrophage colony-stimulating factor (GM-CSF)^{4–6} has been demonstrated in the pathogenesis of psoriasis.⁷ In addition, reports also show the involvement of

Received: February 21, 2020

Accepted: September 3, 2020

Published: September 3, 2020



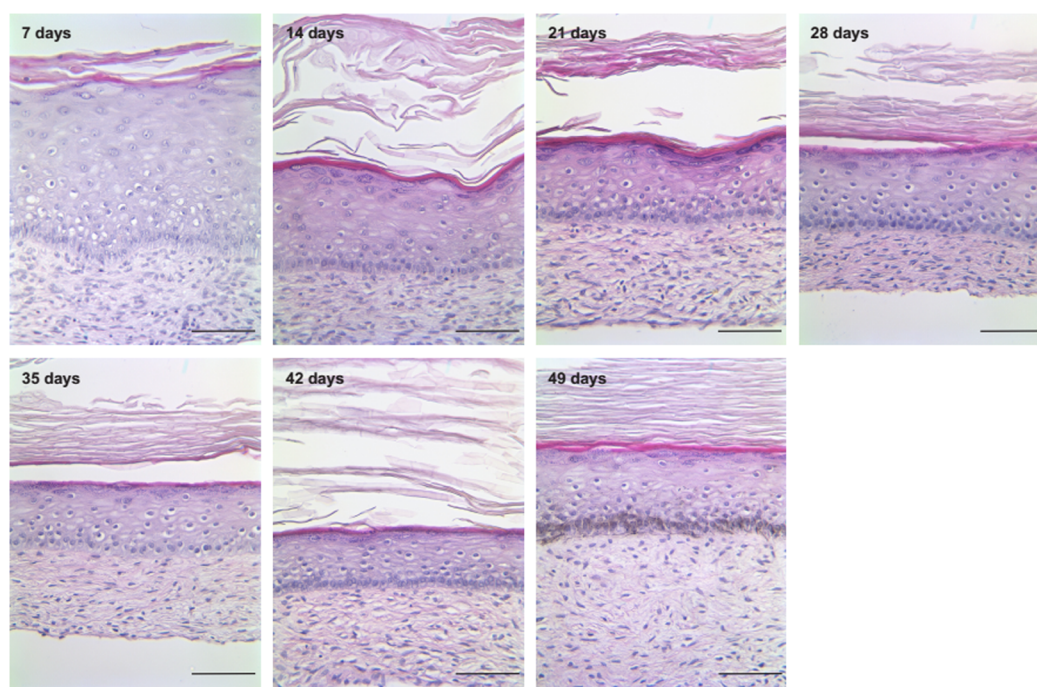


Figure 1. Histological analysis of the developed HSEs up to 7 weeks of culture on the paraffin section. The scale bar represents 100 μm . HSEs older than 28 days are $n = 3$, while models younger than 28 days are $n > 3$.

T_h22 cells in the pathogenesis of psoriasis due to their ample secretion of proinflammatory IL-22.⁸

Beyond affecting the skin, psoriasis exposes the patient to an increased risk of many other diseases like psoriatic arthritis, metabolic syndrome, autoimmune conditions, cardiovascular disease, malignancies, and psychiatric disorders.^{9–11} Thus, psoriasis is a complex and multifactorial disease involving multiple interactions between different cell types and impacts on virtually all aspects of health. Despite the challenges put forward by this debilitating disease, its immune pathogenesis still lacks complete understanding. Therefore, a better understanding of the mechanisms of psoriasis is required so that new therapeutic agents can be developed for better patient outcomes. Over the years, many *in vitro* models of psoriasis are developed to study the pathogenesis of psoriasis and to explore for new therapeutic drug candidates.^{12–15} Currently, the cytokine stimulation approach for developing disease pathogenesis is mainly applied to collagen-based full-thickness skin models. In the collagen models, fibroblasts are embedded in collagen I gels, which function as dermal equivalents.¹⁶ Collagen models can demonstrate characteristic psoriatic phenotypes like epidermal hyperplasia and hypogranulosis and express typical disease markers like HBD-2, SKALP/elafin, and/or S100A7,^{4,17} but these models suffer from poor mechanical strength, contraction, and a limited life span.¹⁸ Typically, these full-thickness skin models start to degrade after approximately 14 days. One of the main causes of the limited life span of these models is the upregulation of collagenase, which deteriorates the existing extracellular matrix (ECM).¹⁹ After stimulation with a disease-specific cytokine cocktail, it generally takes at least 5 days for the development of the disease phenotype like psoriasis.^{4,20} Thus, the relatively short life of the current skin models does not allow testing the treatment/therapy after full development of the disease, thereby failing in mimicking the realistic clinical scenario.

To replicate the clinical drug testing condition on skin models, we can divide the study into three phases. Phase I is the development of the model, phase II is the development of characteristic disease phenotype, and phase III is the start of the treatment protocol. Due to the short longevity of the existing models, mostly phases II and III are combined, which minimizes the duration between the actual disease onset and treatment. Eventually, this can give rise to testing results that do not correlate to the clinical situation. Hence, it is imperative to develop skin models that are viable for long-term treatment. Such models can better mimic clinical situations of diseases such as psoriasis and atopic dermatitis and will enable a time-course study during treatment, equivalent to sequential biopsies. Due to ethical reasons, it is not possible to derive sequential biopsies from patients in clinical studies since biopsies involve the risk of anaphylactic reactions to local anesthesia and always lead to scarring, sometimes even hypertrophic scars or keloids. Therefore, most psoriasis studies often only monitor the clinical condition of the patient (psoriasis area and severity index (PASI) score) and analyze blood samples derived at every patient visit.

Long-term skin models would further assist the development of more complex models with incorporated immune cells and vascularization. A long-term organotypic skin that can accurately model the diseased tissue architecture, with the added potential of the introduction of multiple cell types, however, has not been previously reported.

Different from the approaches used so far, our approach of making a full-thickness skin model is neither based on scaffolds nor hydrogels but instead on the targeted physical modification of cells. In this approach, seeded single cells carry a minimum ECM nanocoating to generate tissue. The approach is based on recent reports by Akashi et al.²¹ who have shown that primary human cells (fibroblast, endothelial, and epithelial cells) equipped with layer-by-layer nanocoating of fibronectin and collagen can (i) spontaneously form 3D tissue and (ii) can be

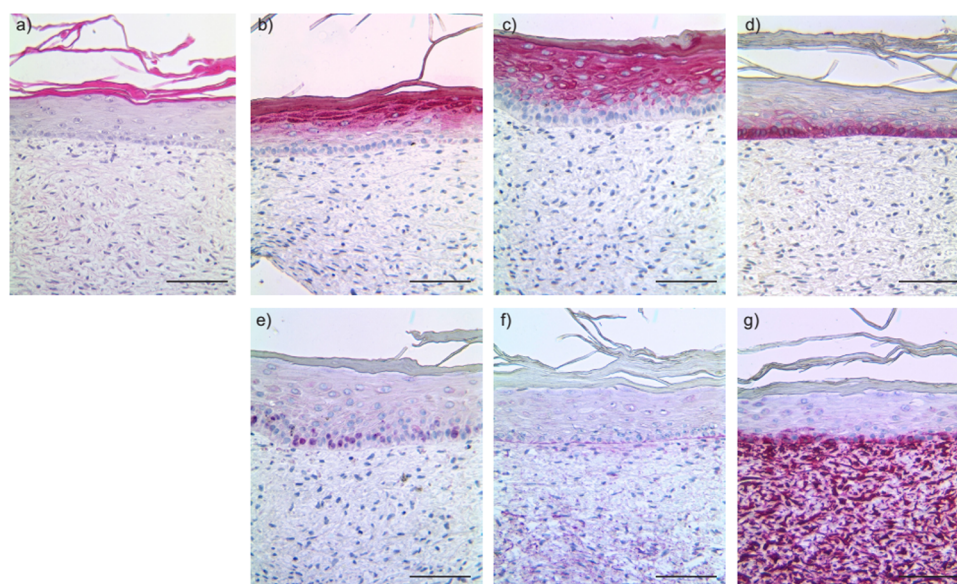


Figure 2. Immunohistological characterization of the HSEs after 3 weeks of cultivation. (a) HE staining. Immunohistochemical staining demonstrates the presence of (b) filaggrin, (c) cytokeratin 10, (d) integrin β , (e) Ki67, (f) collagen IV, and (g) vimentin. Representative images are shown. The scale bar represents 100 μm .

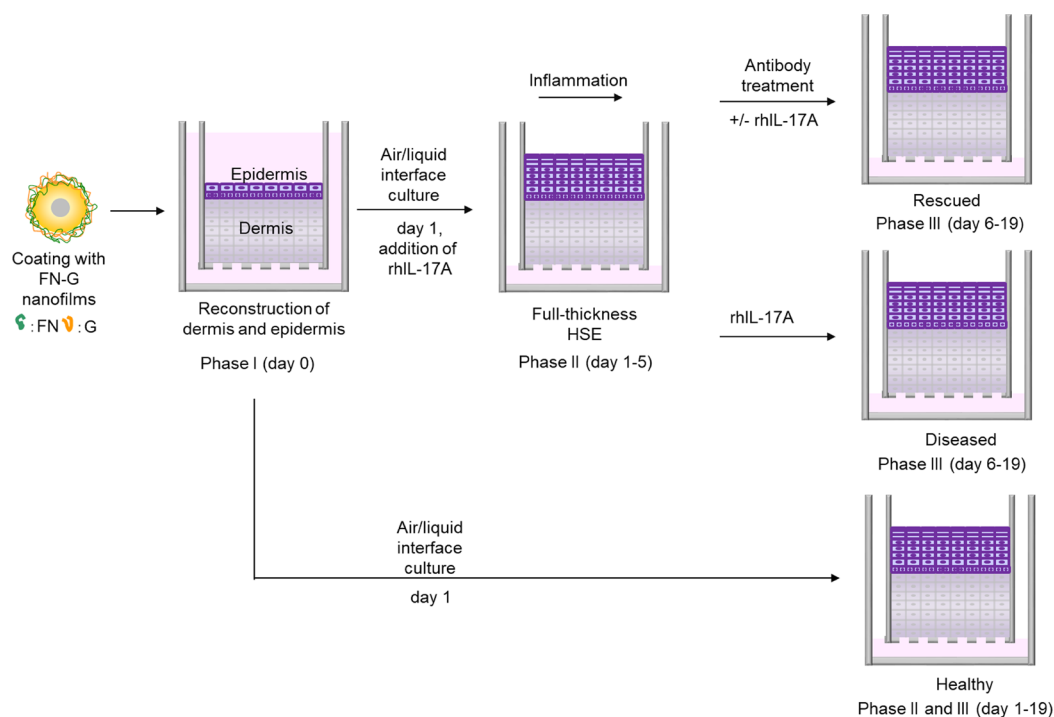
cultivated in hetero-cell cultures. This concept has led to entirely new and extremely promising hetero-cell tissue models in which contacts between different cell types can direct the differentiation from an unstructured cell assembly to an organized and functional microtissue. However, the capability of this technique for long-term skin models has not been explored and such models have never been used to study disease progression and remission. In this study, we could demonstrate the benefits of a long-term HSE to investigate the role of the inflammatory cytokine IL-17A in the pathogenesis of psoriasis and the molecular effects of systemic targeted treatment with secukinumab.

RESULTS AND DISCUSSION

To prepare the HSEs, normal human epithelial keratinocytes (NHEKs) and normal human dermal fibroblasts (NHDFs) were obtained from specimens of cutaneous surgery in healthy volunteers, after informed consent and according to the institutional guidelines and the Declaration of Helsinki principles. The models were prepared using a layer-by-layer coating and accumulation approach.^{21,22} This process is based on preconditioning of cells by ECM proteins, thereby recapitulating the cell adhesive properties of the ECM surrounding cell microenvironment. For fabrication of the models, NHDFs were coated with nanometer-thick fibronectin–gelatin (FN-G) films. The films were coated on the surface of a single cell in a layer-by-layer process (FN-G)₈-FN. After coating, cells were allowed to assemble to form a 3D tissue by cell accumulation in a confined space. This adhesion of the matrix to the cells and itself is solely by integrin binding and protein–protein interaction, equivalent to those present in the natural ECM. For fabrication of the HSEs, 15 layers of coated fibroblasts were assembled on day 1 to form dermis. This was followed by the addition of a monolayer of keratinocytes on day 2. The HSE was introduced to the air–liquid interface (ALI) on day 3 and cultured up to 7 weeks. Histological examination of the HSEs was conducted every week.

Histological examination of the 3D HSEs (Figure 1) revealed a well-stratified epidermis, which is differentiated into four distinct layers—cornified, granular, spinous, and basal. The image clearly shows the formation of a basement membrane separating the homogeneous dermis from the epidermis layers. As expected, the thickness of cornified epidermis was increased with increasing the duration of ALI culture. For the first time, we show that up to 7 weeks, no histological changes owing to the instability of the model could be observed. Staining with Ki67, which is a proliferation marker, further confirmed the viability of the epidermis for the cultured time (Figure S1). Measuring the thickness of the dermis for each time point showed a maximum increase in thickness after 49 days (Figure S2). Additionally, the fibroblast density used to make the model can further augment the ECM production. Conventional collagen gels used for skin models suffer from contraction due to the exertion of traction force by the fibroblasts on local collagen fibers²³ and are prone to degradation by matrix metalloproteases after 2 weeks,²⁴ making them unstable for long-term culture. Contrary to this, FN-G nanofilm coating onto single-cell surfaces promotes the formation of an ECM, while van der Waals interactions and biological recognitions between layers ensure the arrangement of macromolecules in their most stable conformation. The integrins on the cell membrane link the actin cytoskeleton within the cell to external structures in the ECM, allowing cell–cell contact and cell–ECM contact. Based on these characteristics, HSEs that were produced by the cell accumulation technique can be cultivated over a longer period than collagen-based models (Figure S3).

A fine balance between cellular proliferation and differentiation is required to maintain epidermal homeostasis. Therefore, to better characterize the proteins of the epidermis and the dermis, various immunomarkers were used (Figure 2). Filaggrin staining in Figure 2b shows the staining of well-developed keratin fibers in epithelial cells that forms a cornified envelope of stratum corneum. Filaggrin is an S100 fused type of protein essential for epidermal function.^{25,26} Its disruption

Scheme 1. Study Design^a

^aThe study was divided into three phases: The first phase (day 0) comprised the reconstruction of the dermis and epidermis. Within the second phase (days 1–5), HSEs were lifted to the ALI and stimulation with rhIL-17A was conducted. The third phase was divided into three different approaches. While an untreated model served as a control (healthy), one model was stimulated further with rhIL-17A (diseased) and the third model was treated with the anti-IL-17A antibody, with or without rhIL-17A (rescue).

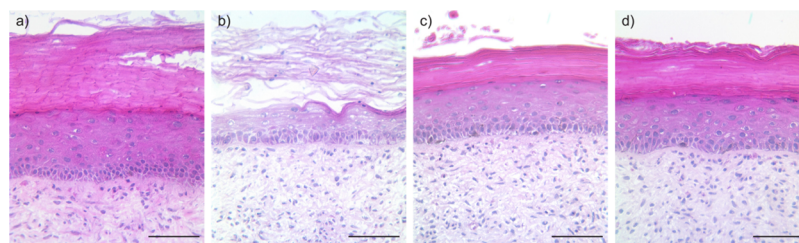


Figure 3. Treatment with an anti-rhIL-17A antibody reverted the cytokine-induced psoriatic phenotype in HSEs. Representative HE images of (a) untreated controls, (b) rhIL17A-stimulated HSEs, (c) HSEs that were stimulated with rhIL-17A for 5 days and then additionally treated with an anti-IL17A-antibody for 14 days (+rhIL17A), and (d) HSEs that were stimulated with rhIL17A for 5 days and then only treated with an anti-IL17A-antibody for 14 days (–rhIL17A). Scale bars: 100 μm

or deficiency leads to abnormal epidermal differentiation and epidermal barrier defects, as seen in the case of atopic dermatitis and psoriasis.^{27,28} Cytokeratin 10 (K10) is the early differentiation marker of keratinocytes. These keratin filaments are present in the intracytoplasmic cytoskeleton of the stratum spinosum of the epithelium (Figure 2c). Integrin $\beta 4$ (ITG $\beta 4$) is a receptor for laminin. It plays a structural role in the cell–cell contact of hemidesmosomes in epithelial cells of the epidermis. ITG $\beta 4$ staining shows the polarizing keratinocytes adjacent to the basement membrane (Figure 2d), while Figure 2e shows the proliferating keratinocytes by Ki67 staining. Figure 2f shows the staining for collagen IV, which is a major component of the basement membrane, while vimentin is the cellular marker for the fibroblast layer (Figure 2g).

To validate the potential applications of the HSE as a disease-specific skin model and as a model for pharmacological examinations, the model was utilized for a study of psoriatic phenotype progression and remission. For disease progression,

rhIL-17A was used, while for disease remission, fully humanized IgG1 κ monoclonal antibody secukinumab was applied. This anti-IL-17A antibody selectively targets IL-17A and blocks its interaction with the IL-17 receptor (IL-17RA/IL-17RC receptor complex).

In the pathogenesis of chronic plaque psoriasis, the cytokine IL-17A functions as an important effector cytokine of the T_H17 cell lineage. It exerts its biologic function through binding to the respective transmembrane IL-17 receptor (IL-17R), which is highly expressed on the surface of keratinocytes. In addition to T cells, IL-17A is also secreted from mast cells and neutrophils during the development of psoriasis.²⁹ This maintains a positive flux for increased production of IL-17A and other mediators involved in the psoriasis gene signature. To model this pathomechanism, after ALI, rhIL-17A was added for 5 days. This was followed by the addition of secukinumab, an antibody against IL-17A, along with the

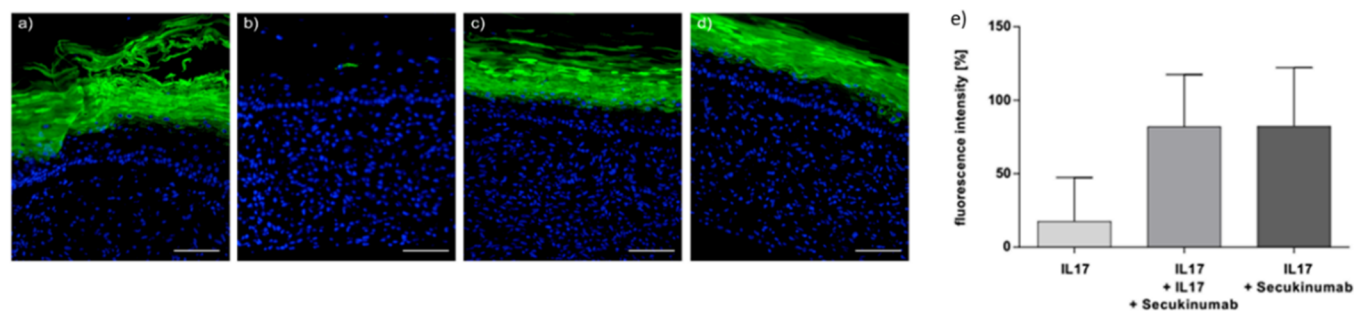


Figure 4. Effects of anti-IL-17A antibody treatment on rhIL-17A-induced impairments were evaluated based on its impact on the filaggrin expression using immunofluorescence staining. (a) Untreated control, (b) rhIL17A-stimulated HSEs, (c) HSEs that were stimulated with rhIL-17A for 5 days and then additionally treated with an anti-IL17A-antibody for 14 days (+rhIL17A), and (d) HSEs that were stimulated with rhIL17A for 5 days and then only treated with an anti-IL17A-antibody for 14 days (−rhIL17A). The scale bar represents 100 μm . (e) Evaluation of fluorescence intensity, normalized to the untreated control. Error bars indicate standard deviation ($n = 3$).

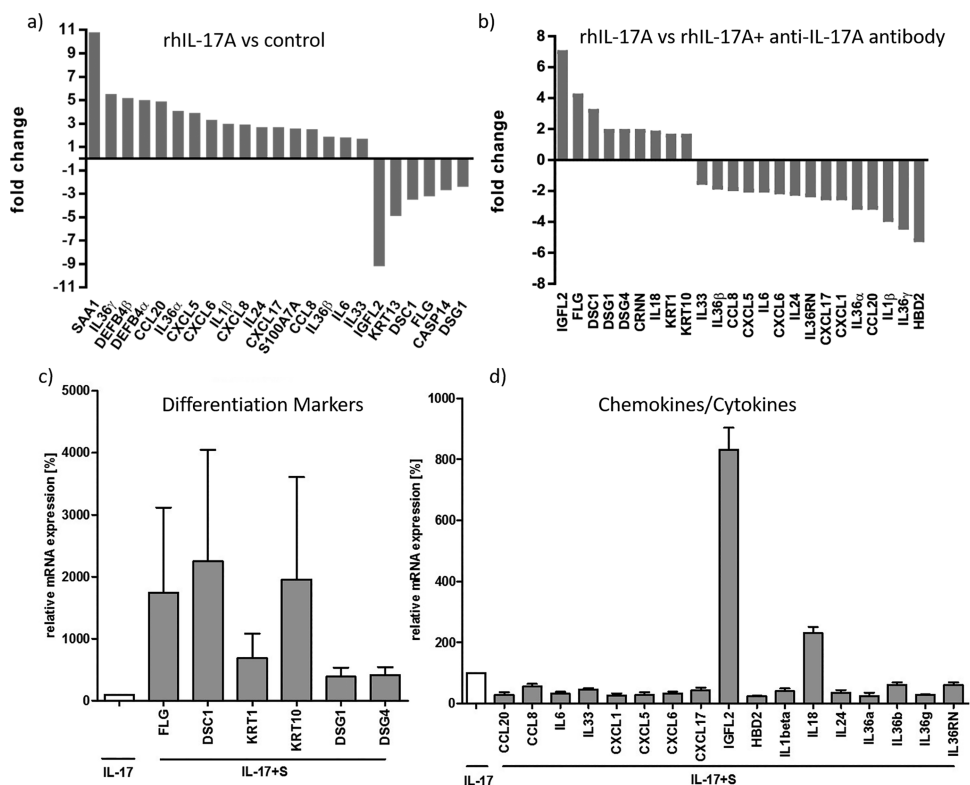


Figure 5. Gene expression profiling. Using microarray analyses, we investigated (a) the effects of rhIL-17A stimulation on HSEs and (b) the effects of treatment with an anti-IL-17A antibody on rhIL17A-stimulated HSEs. RT-PCR analyses confirmed the gene regulations of specific (c) antimicrobial peptides and (d) chemokines and cytokines in HSEs that were treated with the anti-IL17A antibody. S, secukinumab.

addition of rhIL-17A for 14 days (Scheme 1). As controls, we used untreated and rhIL-17A-treated HSEs.

Histological assessment of HSEs treated with rhIL-17A for a total of 19 days demonstrated strong inhibition of keratinocyte differentiation. As a result, hyperproliferative epidermis with premature differentiation of keratinocytes is seen in these models. In psoriatic lesions, the granular layer is reduced and the stratum corneum is formed by incomplete cornified keratinocytes—a phenotype that occurred in the HSEs treated with rhIL-17A (Figure 3b) compared to the non-treated control (Figure 3a). These morphological features of psoriasis were completely negated when the HSEs were treated with anti-IL17A antibody for 14 days with (Figure 3c) or without rhIL-17A (Figure 3d). These results suggest that secukinumab reverts psoriasis-like morphology in HSEs, and for the first

time, we show that the HSEs could be “rescued” after the induction of psoriasis-like phenotype for 14 days along with the antibody. Our characterization of the established HSEs shows that these models can mimic the clinical scenario where $T_{\text{h}}17$ cells in diseased skin constantly produce IL-17 and new biologicals such as an anti-IL17A antibody are administered to achieve therapeutic effects. To show the longevity of models, as a follow-up, the HSEs were treated by rhIL-17A for 5 days followed by the addition of secukinumab for 23 days. It could be seen that the models were stable and were completely recovered from the psoriatic phenotype (Figure S4). This was further confirmed by immunofluorescence staining of CK 6, CK 16, and Ki67 (Figures S5–S7)

The effect of rhIL-17A inhibition on the filaggrin expression was further evaluated using immunofluorescence staining

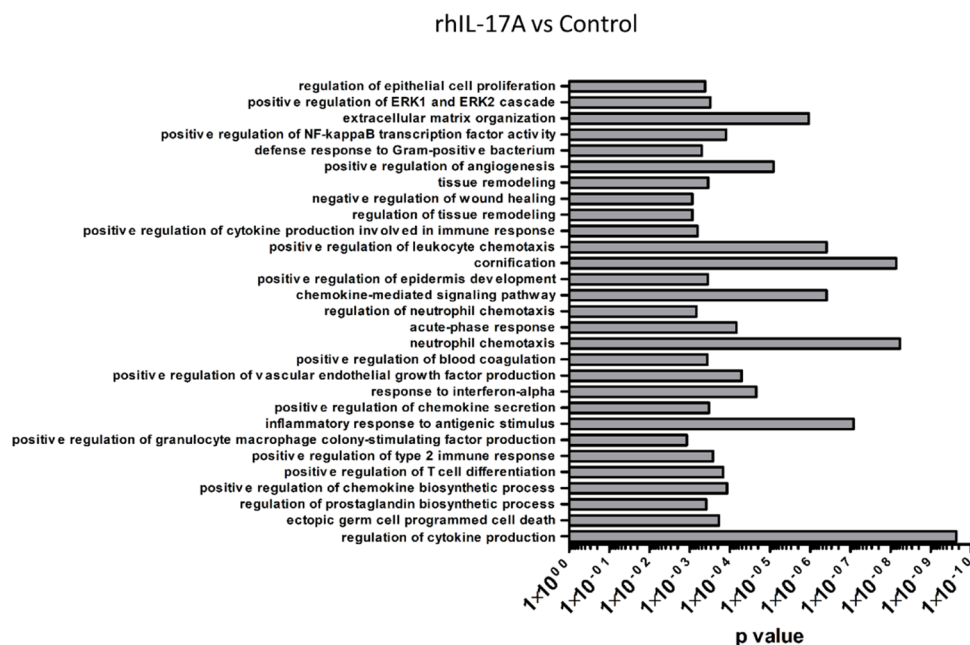


Figure 6. Gene ontology (GO) analysis revealed an impact of rhIL17A on the developed HSEs.

(Figure 4). In psoriasis, late differentiation markers like profilaggrin and loricrin disappear as a result of accelerated keratinization with premature cell death. Additionally, IL-17A down-regulates the expression of filaggrin as well as the genes that encode filaggrin processing and inhibits the expression of tight junction desmosome proteins and the epidermis-associated adhesion molecules such as ZO-1 and ZO-2, E-cadherin, and various integrin molecules. In both models treated with anti-IL17A-antibody for 14 days (+/-rhIL17A), filaggrin expression could be restored (Figure 4c, d, respectively) compared to the rhIL-17A-stimulated models (Figure 4b). The relative fluorescence intensity of both models (Figure 4c,d) was normalized to the untreated control condition (Figure 4a). In the psoriasis-like model, the intensity was reduced to 15% (Figure 4b). However, treatment with anti-IL-17A antibody restored the filaggrin expression up to 80% (Figure 4e) in both models +/-rhIL-17A in phase III. This shows that filaggrin expression could be restored in a psoriasis-like condition using anti-IL-17A antibody, even after the HSEs were continuously subjected to rhIL-17A.

Investigating the molecular effects in more detail, we additionally performed gene expression profiling (Figure 5a,b). Models that were treated with rhIL-17A showed, on the one hand, a downregulation of differentiation markers (e.g., FLG and KRT13) and, on the other hand, an upregulation of chemokines and cytokines (e.g., CXCL5 and IL-36) (Figure 5a). Similar gene regulations can be found in skin lesions of psoriasis patients. Interestingly, treatment with an anti-IL17A antibody reverted these gene regulations only 14 days after initiation of the treatment (Figure 5b). These data demonstrate at the molecular level the “reversing” effects of anti-IL-17A antibody on rhIL-17A-induced gene regulations.

To confirm the microarray data, real-time PCR was performed (Figure 5c, d). In *in vivo*, IL-17A activates CCL20, CXCL1, CXCL2, and CXCL8/IL-8 synthesis, leading to the recruitment of more IL-17-producing T cells and neutrophils into the skin. Thus, blocking IL-17A using anti-IL17A antibody downregulated CXCL1, CXCL2, and CXCL8

and antimicrobial peptides DEFBA- α , DEFBA- β , CCL20 (a chemotactic for T cells and DCs), CCL8, IL-6, and IL-33. IL-36 cytokines are induced in response to IL-17A in HSE, inhibiting IL-17A-downregulated IL-36 expression, which leads to the interruption of a feedback loop of the IL-17 signal pathway, which might explain the rapid onset of the IL-17A antagonist compared to other biologics used in the treatment of psoriasis (anti IL-23 and anti-TNF α).

Interestingly, after treatment with the antibody upregulation of two other markers, IGFL-2 and IL-18 were observed. The potential role of IGFL in psoriasis is not well understood. IGFL proteins demonstrate the closest similarity with IGF family; however, their physiological functions are not defined yet.³⁰ A former study revealed that IGFL-2 downregulation is detected in skin samples of psoriasis patients.³¹ Interestingly, treatment of the psoriasis-like HSE with secukinumab led to a significant upregulation of IGFL-2 expression. Its structural similarity to IGF family suggests that these proteins could act as growth regulators, and hence understanding its role in the pathogenesis of psoriasis may further give an insight into its role in the pathogenesis of psoriasis and its treatment.³²

Keratinocytes in all living layer of epidermis show the presence of IL-18 and its receptors. The release of IL-18 affects the surrounding keratinocytes in an autocrine and paracrine manner. In normal skin, this results in preserving the homeostasis of a T_H1-dominant state.³³ However, psoriasis-like symptoms are aggravated in the combination of IL-18 with IL-17.³³ We assume that the addition of rhIL-17A further upregulates the IL-18 production in our model and blocking rhIL-17A mechanistically did not influence IL-18 regulation. Further dynamics of IL-18 and the IL-18 receptor in diseased skin as compared to normal skin have to be investigated to have a better insight.

Gene ontology (GO) analysis revealed an impact of rhIL17A on biological processes such as “regulation of epithelial cell proliferation”, “positive regulation of cytokine production involved in immune response”, and “positive regulation of chemokine secretion” (Figure 6). These data substantiate the

proinflammatory and chemotactic effects of rhIL17A on the established HSEs.

CONCLUSIONS

We used the cell coating technique to fabricate the 3D skin equivalents. This technique involves layer-by-layer assembly of extracellular matrix nanofilms on the cell surface and allows the rapid fabrication of scaffold-free skin models. After lifting the model to the air–liquid interface on day 3, keratinocytes as a major cell population showed homogeneous differentiation into four layers on the surface of the dermis. Histological examination revealed a stable skin equivalent in long-term cell culture (49 days), and this is beyond any reported state of the art.

Owing to the long-term stability of the skin models, we further developed a 3D psoriatic skin model that mimics the clinical psoriatic phenotype. The pilot study consisted of inducing the psoriasis phenotype by stimulation of the skin equivalents with 50 ng/mL rhIL-17A for 5 days followed by a systemic treatment from day 6 to day 19 with the monoclonal antibody secukinumab along with rhIL-17A. After treatment with an anti-IL7A antibody, upregulation of keratinocyte differentiation markers such as FLG, KRT1, KRT10, DSG1, and DSG4 and downregulation of antimicrobial peptides such as DEFB4B and DEFB4A (HBD-2) were observed. Inhibiting rhIL-17A also downregulated CCL20 (a chemotactic for T cells and DCs), CCL8, CXCL1, CXCL2, CXCL8, IL-6, IL-33, and IL-36. To conclude, we could induce a psoriatic-like disease phenotype in a 3D organotypic skin model and showed the restoration of the model by antibody treatment. For the first time, the performed study aimed at mimicking the clinical situation in psoriasis. In the next step, we plan to induce the psoriasis phenotype for 5 days followed by 14 days of treatment with biologicals and then withdraw the treatment and monitor the washout phase for an additional 14 days. Furthermore, we know from our clinical practice that, especially, laser and aesthetic treatments reveal clinical effects up to 2 months after treatment, and these effects can only be monitored in a long-term 3D skin model. We contemplate the use of developed skin models as an alternative to diseased tissue biopsies and animal testing.

MATERIALS AND METHODS

Materials. Normal human epithelial keratinocytes (NHEK) and normal human dermal fibroblasts (NHDF) were isolated and cultured as previously described.³⁴ NHEKs and NHDFs were obtained from foreskin or specimens from cutaneous surgery in healthy subjects, after informed consent and according to the institutional guidelines and the Declaration of Helsinki principles. The ethics committee of the University Hospital, RWTH Aachen, Germany, approved this study.

3D Human Skin Equivalents. Individual fibroblast cells were ECM-coated with fibronectin (FN) and gelatin (G) as previously described.²¹ Briefly, dermal fibroblasts were trypsinized, centrifuged, washed with PBS, and mixed with 0.04 $\mu\text{g}/\text{mL}$ FN and 0.04 $\mu\text{g}/\text{mL}$ G with an intermediate PBS washing step. After each mixing step, the cells were centrifuged for 1 min at 400g. A total of nine coating steps were performed. Coated fibroblasts were then seeded inside 6.5 mm trans-well inserts with 0.4 μm pore size. We used a total of 1.5×10^6 and 0.5×10^6 coated NHDFs for 15 layers and 5 layers of dermis, respectively. The NHDFs were used from passage 4–9. The formed dermis was incubated for 24 h (37 °C, 5% CO₂) with DMEM, 1% penstrep, and 5% FBS before the addition of human keratinocytes. The next day, 1.8×10^5 keratinocytes in 300 μL of keratinocyte media (DermaLife K Serum-Free Keratinocyte Culture Medium) were

seeded on top of the formed dermis layer. The lower compartment of the trans-well was filled with 1 mL media. The construct was incubated for 2 h at 37 °C and 5% CO₂ to allow optimal attachment of keratinocytes to the dermal compartment. After the incubation time, the media from the outer and inner parts of the trans-well inserts were extracted and 2.3 mL of fresh growth media (Dermalife K serum-free keratinocytes medium/DMEM (50:50), 0.5% penstrep, and FBS 5%) was added. The models were incubated for 24 h. The next day, media from the well plate were extracted and the outer compartment of the trans-well was filled with 1 mL of differentiation media (Dermalife without TGF alpha/DMEM (50:50), FBS 5%, 0.5% penstrep, 1 mM CaCl₂, and 50 $\mu\text{g}/\text{mL}$ ascorbic acid), whereas no media was added on the inner compartment. The models were cultured in ALI for 7 weeks with media changes every alternate day.

Psoriasis-like skin conditions were generated by adding rhIL-17A (50 ng/mL, Peprotech) to the basolateral compartment when models were lifted to the air–liquid interface. 3D models were stimulated for a total of 19 days. To assess the impact of secukinumab, 3D models were concurrently treated with secukinumab (6 $\mu\text{g}/\text{mL}$ in dimethylsulfoxide (DMSO) and rhIL-17A (50 ng/mL)). 3D skin cultures were harvested 19 days after stimulation with the cytokine and rhIL17A with or without pretreatment of 5 days with rhIL17A. The culture medium was changed, and stimulation was repeated every other day. To ensure reproducible results, all experiments were performed in triplicate.

Collagen-Based HSE. Collagen-based full-thickness 3D skin equivalents were constructed as described previously.³⁵ In brief, to establish the dermal part of the skin equivalents, ice-cold bovine collagen I solution (Vitrogen, Cohesion Technologies, Palo Alto, CA, USA) and 10 \times concentrated Hank's balanced salt solution (Gibco/Invitrogen, Darmstadt, Germany) were mixed in 8:1 by volume ratio. This was neutralized with 1 M NaOH followed by addition of one volume of FCS containing 1×10^6 NHDFs. Four milliliters of this solution (4×10^5 cells) was seeded into polycarbonate cell culture inserts for a six-well plate (3 μm pore size, Nunc; Thermo Fisher Scientific, Langensfeld, Germany). The dermal equivalent was seeded with 1×10^6 NHEKs after 2 days and submerged in equal volumes of DMEM and keratinocyte growth medium (Dermalife K serum-free keratinocytes medium) with 5% FCS, 50 μg of ascorbic acid, and 5 $\mu\text{g}/\text{mL}$ aprotinin (Applichem, Chicago, IL, USA). On day 3, the HSEs were lifted to the air–liquid interface.

RNA Isolation. Total RNA was isolated from psoriasis-like 3D skin models. Whole tissue was lysed with a tissue lyzer II (Quiagen) in lysis buffer of nucleospin RNA kit (Macherey-Nagel, Duren, Germany), according to the manufacturer's instructions. The quantity of the RNA was measured (NanoDrop Technologies, Wilmington, DE, USA), and the integrity was confirmed (Agilent 2100 Bioanalyzer; Agilent Technologies, Palo Alto, CA, USA).

Quantitative Real-Time PCR. Purified RNA was reverse-transcribed into cDNA using the SuperScript VILO Mastermix (Life Technologies, Langensfeld, Germany), according to the manufacturer's instructions. Quantitative real-time (qRT) PCR analyses were performed on an ABI Prism 7300 Sequence Detection System (Applied Biosystems, Weiterstadt, Germany) using Assays-on-Demand gene expression products (Applied Biosystems) for human CCL8 (HS00271615_m1), CCL20 (HS01011368_m1), CXCL1 (HS00236937_m1), CXCL5 (HS00171085_m1), CXCL6 (HS00605742_g1), CXCL17 (HS01650998_m1), CRNN (HS00211833_m1), FLG (HS00856927_g1), DSC1 (HS00245189_m1), DSG1 (HS00355084_m1), DSG4 (HS01125472_m1), IL-1beta (HS00174097_m1), IL-6 (HS00985641_m1), IL-18 (HS01038788_m1), IL-24 (HS01114274_m1), IL-33 (HS01125943_m1), IL-36alpha (HS00205367_m1), IL-36beta (HS00758166_m1), IL-36gamma (HS00219742_m1), IL36RN (HS00202179_m1), IGFL-2 (HS03645208_m1), KRT1 (HS01549614_g1), and KRT10 (HS00166289_m1), according to the manufacturer's recommendations. An Assays-on-Demand product for HPRT (Hs99999909_m1) was used as an internal standard.

Microarray Analysis. For microarray analysis, purified mRNA was amplified, labeled, and hybridized to Human Clariom S Array, according to the manufacturer's instructions as previously described.³⁴ Data were analyzed using GeneSpring GX 14.9 software (Agilent Technologies, Frankfurt am Main, Germany). Gene ontology enrichment analysis was performed using <http://www.geneontology.org/>.

Light Microscopy, Immunofluorescence, and Immunohistochemistry. The tissues were either fixed in 10% formalin for paraffin embedding or embedded in Tissue Tek O.C.T. for cryosections. For light microscopy, 4 μm paraffin sections of 3D models were stained with hematoxylin and eosin (H&E). For immunohistochemistry, paraffin-embedded tissue was cut into 4 μm sections, mounted on Superfrost slides (Menzel, Braunschweig, Germany), deparaffinized, and rehydrated. To unmask antigens, the specimens were treated with "Target Retrieval Solution Citrate" (pH 6.0, Dako), according to the manufacturer's instructions, and rinsed in distilled water. Specimens were incubated for 60 min with primary mouse anti-human monoclonal antibodies: filaggrin (clone AKH1, 1:100; Santa Cruz Biotech, Santa Cruz, USA), cytokeratin 10 (1:500), Ki67 (1:50), collagen IV (1:50; Dako Glostrup, Denmark), integrin $\beta 4$ (1:200; Abcam, Cambridge, UK), and vimentin (1:200; Sigma Aldrich, Missouri, USA). Binding of the antibodies was visualized by the Dako "Real Detection System Alkaline Phosphatase/RED" on a universal staining system (Dako), as specified by the manufacturer. Finally, specimens were counterstained with hematoxylin and mounted with coverslips. For immunofluorescence, 4 μm cryosections were fixed in acetone and incubated for 1 h with primary antibodies as described above. Goat anti-mouse IgG Alexa Fluor 488-conjugated secondary antibody (Molecular Probes, Eugene, OR, USA) was added for epifluorescence detection using a Leica DM IL photomicroscope (Leica Microsystems, Wetzlar, Germany) with digital photo documentation (DISKUS; Hilgers, Königswinter, Germany).

The illustrations used in the publication were created with BioRender.com

■ ASSOCIATED CONTENT

SI Supporting Information

The Supporting Information is available free of charge at <https://pubs.acs.org/doi/10.1021/acsabm.0c00202>.

Ki67 staining of HSEs at different time points, thickness index of the dermis, comparison of HSE prepared using cell coating to collagen-based HSE, histological analysis, and CK 6, CK 16, and Ki67 immunofluorescence staining of 28 day psoriatic HSEs (PDF)

■ AUTHOR INFORMATION

Corresponding Authors

Smriti Singh – DWI-Leibniz Institute for Interactive Materials, Aachen S2074, Germany; orcid.org/0000-0002-2164-9912; Email: singh@dwil.rwth-aachen.de

Jens M. Baron – Department of Dermatology and Allergology, University Hospital, RWTH Aachen University, Aachen S2074, Germany; Email: jbaron@ukaachen.de

Authors

Yvonne Marquardt – Department of Dermatology and Allergology, University Hospital, RWTH Aachen University, Aachen S2074, Germany

Rahul Rimal – DWI-Leibniz Institute for Interactive Materials, Aachen S2074, Germany; orcid.org/0000-0003-0923-480X

Akihiro Nishiguchi – DWI-Leibniz Institute for Interactive Materials, Aachen S2074, Germany; Research Center for Functional Materials, National Institute for Materials Science,

Tsukuba, Ibaraki 305-0044, Japan; orcid.org/0000-0002-3160-6385

Sebastian Huth – Department of Dermatology and Allergology, University Hospital, RWTH Aachen University, Aachen S2074, Germany

Mitsuru Akashi – Graduate School of Frontier Biosciences, Osaka University, Osaka 565-0871, Japan

Martin Moeller – DWI-Leibniz Institute for Interactive Materials, Aachen S2074, Germany; A.N. Nesmeyanov Institute of Organoelement Compounds of Russian Academy of Science, Moscow 119991, Russia; orcid.org/0000-0002-5955-4185

Complete contact information is available at: <https://pubs.acs.org/doi/10.1021/acsabm.0c00202>

Author Contributions

S.S., M.M., and J.M.B. conceived the idea and supervised the project. S.S., Y.M., R.R., and A.N. did the experiments. S.S., S.H., and J.M.B. interpreted the data, and S.S., S.H., and J.M.B. wrote the manuscript.

Notes

The authors declare no competing financial interest.

■ ACKNOWLEDGMENTS

Financial support from DWI-Förderverein is highly acknowledged. M.M. gratefully acknowledges the support of an advanced grant from the European Research Council (ERC), Jellyclock 695716, and grant of the government of the Russian federation no. 14.W03.31.0018. This work was also performed in part at the Center for Chemical Polymer Technology CPT, which was supported by the EU and the federal state of North Rhine-Westphalia (grant EFRE 30 00883 02).

■ ABBREVIATIONS

FLG, filaggrin; DSC1, desmocollin1; DSG1, desmoglein1; DSG4, desmoglein 4; IGFL2, insulin growth factor-like family member 2; IGF, insuline-like growth factor; KRT1, keratin1, type I; KRT10, keratin10, type I; IL-1B, interleukin 1beta; rhIL-17A, recombinant human interleukin17A; IL-17, interleukin 17; IL-18, interleukin 18; IL-24, interleukin 24; IL-36 α , interleukin 36 alpha; IL-36 β , interleukin 36 beta; IL-36 γ , interleukin 36 gamma; IL36RN, interleukin 36 receptor antagonist; CCL8, chemokine(C-C motif) ligand 8; CCL20, chemokine(C-Cmotif) ligand 20; CXCL1, chemokine(C-X-C motif) ligand 1; CXCL5, chemokine(C-X-C motif) ligand 5; CXCL6, chemokine(C-X-C motif) ligand 6; CXCL17, chemokine(C-X-C motif) ligand 17

■ REFERENCES

- (1) Pittelkow, M. R. Psoriasis: more than skin deep. *Nat. Med.* **2005**, *11*, 17–18.
- (2) Greb, J. E.; Goldminz, A. M.; Elder, J. T.; Lebwohl, M. G.; Gladman, D. D.; Wu, J. J.; Mehta, N. N.; Finlay, A. Y.; Gottlieb, A. B. Psoriasis. *Nat. Rev. Dis. Primers* **2016**, *2*, 16082.
- (3) Lowes, M. A.; Suárez-Fariñas, M.; Krueger, J. G. Immunology of psoriasis. *Annu. Rev. Immunol.* **2014**, *32*, 227–255.
- (4) Pfaff, C. M.; Marquardt, Y.; Fietkau, K.; Baron, J. M.; Lüscher, B. The psoriasis-associated IL-17A induces and cooperates with IL-36 cytokines to control keratinocyte differentiation and function. *Sci. Rep.* **2017**, *7*, 15631.
- (5) Ma, W.-Y.; Jia, K.; Zhang, Y. IL-17 promotes keratinocyte proliferation via the downregulation of C/EBP α . *Exp. Ther. Med.* **2016**, *11*, 631–636.

- (6) Eberle, F. C.; Brück, J.; Holstein, J.; Hirahara, K.; Ghoreschi, K. Recent advances in understanding psoriasis. *F1000Res* **2016**, *5*, 770.
- (7) Lowes, M. A.; Kikuchi, T.; Fuentes-Duculan, J.; Cardinale, I.; Zaba, L. C.; Haider, A. S.; Bowman, E. P.; Krueger, J. G. Psoriasis Vulgaris Lesions Contain Discrete Populations of Th1 and Th17 T Cells. *J. Invest. Dermatol.* **2008**, *128*, 1207–1211.
- (8) Ramirez, J.-M.; Brembilla, N. C.; Sorg, O.; Chicheportiche, R.; Matthes, T.; Dayer, J.-M.; Saurat, J.-H.; Roosnek, E.; Chizzolini, C. Activation of the aryl hydrocarbon receptor reveals distinct requirements for IL-22 and IL-17 production by human T helper cells. *Eur. J. Immunol.* **2010**, *40*, 2450–2459.
- (9) Neimann, A. L.; Shin, D. B.; Wang, X.; Margolis, D. J.; Troxel, A. B.; Gelfand, J. M. Prevalence of cardiovascular risk factors in patients with psoriasis. *J. Am. Acad. Dermatol.* **2006**, *55*, 829–835.
- (10) Abuabara, K.; Azfar, R. S.; Shin, D. B.; Neimann, A. L.; Troxel, A. B.; Gelfand, J. M. Cause-specific mortality in patients with severe psoriasis: a population-based cohort study in the U.K. *Br. J. Dermatol.* **2010**, *163*, 586–592.
- (11) Korman, N. J.; Zhao, Y.; Pike, J.; Roberts, J. Relationship between psoriasis severity, clinical symptoms, quality of life and work productivity among patients in the USA. *Clin. Exp. Dermatol.* **2016**, *41*, 514–521.
- (12) Desmet, E.; Ramadhas, A.; Lambert, J.; Van Gele, M. In vitro psoriasis models with focus on reconstructed skin models as promising tools in psoriasis research. *Exp. Biol. Med.* **2017**, *242*, 1158–1169.
- (13) Roy, B.; Simard, M.; Lorthois, I.; Bélanger, A.; Maheux, M.; Duque-Fernandez, A.; Rioux, G.; Simard, P.; Deslauriers, M.; Masson, L.-C.; Morin, A.; Pouliot, R. In vitro models of psoriasis. In *Skin Tissue Models*; Marques, A. P.; Pirraco, R. P.; Cerqueira, M. T.; Reis, R. L., Eds. Academic Press: Boston, 2018; pp. 103–128.
- (14) Niehues, H.; van den Bogaard, E. H. Past, present and future of in vitro 3D reconstructed inflammatory skin models to study psoriasis. *Exp. Dermatol.* **2018**, *27*, 512–519.
- (15) Smits, J. P. H.; Niehues, H.; Rikken, G.; van Vlijmen-Willems, I. M. J. J.; van de Zande, G. W. H. J. F.; Zeeuwen, P. L. J. M.; Schalkwijk, J.; van den Bogaard, E. H. Immortalized N/TERT keratinocytes as an alternative cell source in 3D human epidermal models. *Sci. Rep.* **2017**, *7*, 11838.
- (16) Pfaff, C. M.; Kluwig, D.; Marquardt, Y.; Fietkau, K.; Lüscher, B.; Baron, J. M. 301 The psoriasis-associated IL-17A induces and cooperates with IL-36 cytokines to control keratinocyte differentiation and function. *J. Invest. Dermatol.* **2017**, *137*, S244.
- (17) Pfaff, C. M.; Marquardt, Y.; Czaja, K.; Lüscher, B.; Baron, J. M. 309 The psoriasis-associated IL-17A interferes with keratinocyte differentiation and skin barrier formation in 3D skin models. *J. Invest. Dermatol.* **2016**, *136*, S55.
- (18) Feng, Z.; Yamato, M.; Akutsu, T.; Nakamura, T.; Okano, T.; Umezumi, M. Investigation on the mechanical properties of contracted collagen gels as a scaffold for tissue engineering. *Artif. Organs* **2003**, *27*, 84–91.
- (19) Tandara, A. A.; Mustoe, T. A. MMP- and TIMP-secretion by human cutaneous keratinocytes and fibroblasts – impact of coculture and hydration. *J. Plast., Reconstr. Aesth. Surg.* **2011**, *64*, 108–116.
- (20) Clarysse, K.; Pfaff, C. M.; Marquardt, Y.; Huth, L.; Kortekaas Krohn, I.; Kluwig, D.; Lüscher, B.; Gutermuth, J.; Baron, J. JAK1/3 inhibition preserves epidermal morphology in full-thickness 3D skin models of atopic dermatitis and psoriasis. *J. Eur. Acad. Dermatol. Venereol.* **2019**, *33*, 367–375.
- (21) Nishiguchi, A.; Yoshida, H.; Matsusaki, M.; Akashi, M. Rapid construction of three-dimensional multilayered tissues with endothelial tube networks by the cell-accumulation technique. *Adv. Mater.* **2011**, *23*, 3506–3510.
- (22) Matsusaki, M.; Fujimoto, K.; Shirakata, Y.; Hirakawa, S.; Hashimoto, K.; Akashi, M. Development of full-thickness human skin equivalents with blood and lymph-like capillary networks by cell coating technology. *J. Biomed. Mater. Res. Part A* **2015**, *103*, 3386–3396.
- (23) Moulin, V.; Castilloux, G.; Jean, A.; Garrel, D. R.; Auger, F. A.; Germain, L. In vitro models to study wound healing fibroblasts. *Burns* **1996**, *22*, 359–362.
- (24) Karsdal, M. A.; Nielsen, S. H.; Leeming, D. J.; Langholm, L. L.; Nielsen, M. J.; Manon-Jensen, T.; Siebuhr, A.; Gudmann, N. S.; Rønnow, S.; Sand, J. M.; Daniels, S. J.; Mortensen, J. H.; Schuppan, D. The good and the bad collagens of fibrosis - Their role in signaling and organ function. *Adv. Drug Delivery Rev.* **2017**, *121*, 43–56.
- (25) Dale, B. A.; Resing, K. A.; Lonsdale-Eccles, J. D. Filaggrin: A Keratin Filament Associated Proteina. *Ann. N. Y. Acad. Sci.* **1985**, *455*, 330–342.
- (26) Brown, S. J.; Irwin McLean, W. H. One Remarkable Molecule: Filaggrin. *J. Invest. Dermatol.* **2012**, *132*, 751–762.
- (27) Pendaries, V.; Malaise, J.; Pellerin, L.; Le Lamer, M.; Nachat, R.; Kezic, S.; Schmitt, A.-M.; Paul, C.; Poumay, Y.; Serre, G.; Simon, M. Knockdown of Filaggrin in a Three-Dimensional Reconstructed Human Epidermis Impairs Keratinocyte Differentiation. *J. Invest. Dermatol.* **2014**, *134*, 2938–2946.
- (28) Yoneda, K.; Nakagawa, T.; Lawrence, O. T.; Huard, J.; Demitsu, T.; Kubota, Y.; Presland, R. B. Interaction of the Profilaggrin N-Terminal Domain with Loricrin in Human Cultured Keratinocytes and Epidermis. *J. Invest. Dermatol.* **2012**, *132*, 1206–1214.
- (29) Lin, A. M.; Rubin, C. J.; Khandpur, R.; Wang, J. Y.; Riblett, M.; Yalavarthi, S.; Villanueva, E. C.; Shah, P.; Kaplan, M. J.; Bruce, A. T. Mast Cells and Neutrophils Release IL-17 through Extracellular Trap Formation in Psoriasis. *J. Immunol.* **2011**, *187*, 490–500.
- (30) Emtage, P.; Vatta, P.; Arterburn, M.; Muller, M. W.; Park, E.; Boyle, B.; Hazell, S.; Polizotto, R.; Funk, W. D.; Tang, Y. T. IGFL: A secreted family with conserved cysteine residues and similarities to the IGF superfamily. *Genomics* **2006**, *88*, 513–520.
- (31) Lobito, A. A.; Ramani, S. R.; Tom, I.; Bazan, J. F.; Luis, E.; Fairbrother, W. J.; Ouyang, W.; Gonzalez, L. C. Murine insulin growth factor-like (IGFL) and human IGFL1 proteins are induced in inflammatory skin conditions and bind to a novel tumor necrosis factor receptor family member, IGFLR1. *J. Biol. Chem.* **2011**, *286*, 18969–18981.
- (32) Edmondson, S. R.; Thumiger, S. P.; Werther, G. A.; Wraight, C. J. Epidermal homeostasis: the role of the growth hormone and insulin-like growth factor systems. *Endocr. Rev.* **2003**, *24*, 737–764.
- (33) Lee, J. H.; Cho, D. H.; Park, H. J. IL-18 and Cutaneous Inflammatory Diseases. *Int. J. Mol. Sci.* **2015**, *16*, 29357–29369.
- (34) Schmitt, L.; Marquardt, Y.; Heise, R.; von Felbert, V.; Amann, P. M.; Huth, L.; Steiner, T.; Hölzle, F.; Huth, S.; Baron, J. M. Novel Human Full-Thickness Three-Dimensional Nonkeratinized Mucous Membrane Model for Pharmacological Studies in Wound Healing. *Skin Pharmacol. Physiol.* **2019**, *32*, 265–274.
- (35) Marquardt, Y.; Amann, P. M.; Heise, R.; Czaja, K.; Steiner, T.; Merk, H. F.; Skazik-Voogt, C.; Baron, J. M. Characterization of a novel standardized human three-dimensional skin wound healing model using non-sequential fractional ultrapulsed CO2 laser treatments. *Lasers Surg. Med.* **2015**, *47*, 257–265.